JOURNAL OF MATERIALS SCIENCE **40** (2005) 5933–5939

Finite element modelling of rubber-like materials — a comparison between simulation and experiment

M. BÖL*, S. REESE
Institute of Mechanics, Department of Civil Engineering, Ruhr University Bochum, Universitätsstraße 150, D-44801 Bochum, Germany
E-mail: boel@nm.ruhr-uni-bochum.de

In this work finite element simulations are used based on the micro structure of polymers in order to transfer the information of the micro level to the macro level. The microscopic structure of polymers is characterized by a three-dimensional network consisting of randomly oriented chain-like macromolecules linked together at certain points. Different techniques are used to simulate the rubber-like material behaviour of such networks. These techniques range from molecular dynamics to the finite element method.

The proposed approach is based on a so-called unit cell. This unit cell consists of one tetrahedral element and six truss elements. To each edge of the tetrahedron one truss element is attached which models the force-stretch behaviour of a bundle of polymer chains. The proposed method provides the possibility to observe how changes at the microscopic level influence the macroscopic material behaviour. Such observations were carried out in [1]. The main focus of this work is the validation of the proposed approach. Therefore the model is compared to different experimental data and other statistically-based network models describing rubber-like material behaviour.

1. Introduction

One characteristic of polymers is their microscopic structure which consists of long, randomly oriented molecule chains. These chains are linked together at certain points. In this way an arbitrary three-dimensional network is formed. There exist different interactions between the particular atoms (see e.g. [2–4]).

Several authors have studied the micro mechanical behaviour by means of molecular dynamics simulations (cp. [5–7]). These approaches, based on techniques such as the Monte Carlo method or the bond fluctuation method, have in common that in the discretized model each chain or even chain link is represented separately. In this way for instance the vulcanization process can be modelled very realistically. However, such simulations require an extreme computational effort.

Using the tool of statistical mechanics the numerical modelling can be noticeably simplified (see e.g. [8–13]). Based on the assumption that the bonds of the network are permanent these latter concepts use the following four assumptions. First of all, all chains of the network have the same length $n\ l$ in the totally extended state (n number of chain links, l average length of a chain link). Secondly, the distribution of the end-to-end distances r of the chains is calculated by means of Gaussian statistics. Thirdly, the deformation of the material is affine and fourthly there is no change in volume. Following these assumptions Treloar [12] and [13] derived the well-known "Neo-Hookean" free energy function (per reference volume) $W = (\mu/2)\,(\lambda_1^2+\lambda_2^2+\lambda_3^2-3)$ for moderate strains where λ_i $(i = 1, 2, 3)$ represent the principal stretches and $\mu = N\,k\,\Theta$ denotes the rubber shear modulus (N number of chains per reference volume, k Boltzmann's constant, Θ absolute temperature). More recent models (cp. [14–17]) are able to predict the material response also for higher strains. The mentioned concepts are based on the Langevin statistics which was originally suggested by [18]. However, also the more recent network theories work with the first, the third and the fourth assumption.

Alternatively rubber-like materials can be described by phenomenological models, see [19–22]. The best agreement with experiments is displayed by the model of Swanson [22] which, however, needs 16 parameters. The disadvantage of the continuum-based models with respect to the models based on chain statistics lies in the fact that the material parameters are not physically

*Author to whom all correspondence should be addressed.
0022-2461
DOI: 10.1007/s10853-005-5058-x

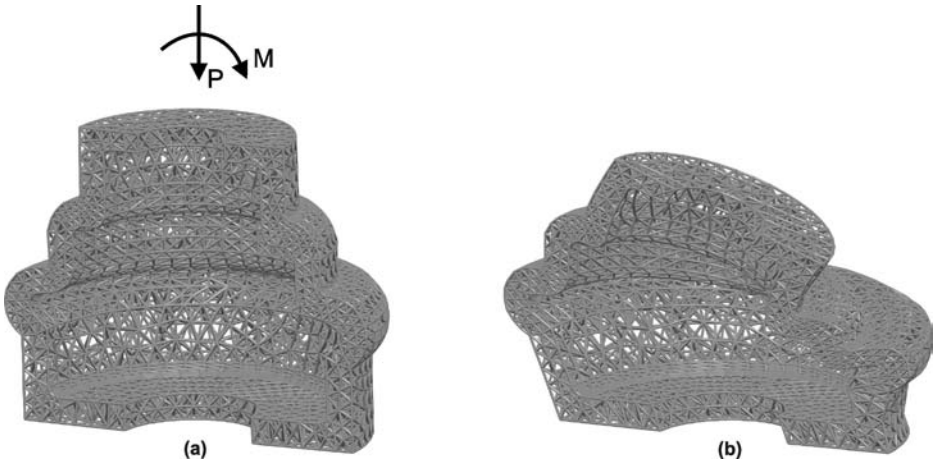

Figure 1 Rubber boot of a joint: (a) meshed geometry (truss elements only), (b) deformed mesh.

motivated. As such they can only be found by means of experiments. This fitting procedure can be very elaborate if the number of parameters is large.

To overcome these problems in the present contribution a micro mechanically-based approach is preferred. In comparison to earlier works we aim to avoid the four assumptions mentioned before. The transfer of the known micro mechanical information about the material to the macroscopic level by means of the finite element method is crucial to the work.

In the present approach the microscopic structure of polymers is represented by an assembly of non-linear truss elements. Each truss element models the micro mechanical force-stretch behaviour of a certain group of chains. With six of them and one tetrahedral element we establish a so-called unit cell in such a way that the truss elements lie on the edges of the tetrahedral element. The tetrahedral element serves to model the hydrostatic pressure built up in one unit cell. Using a random assembling procedure by help of a random generator we are in a position to model arbitrary geometries. Another possibility to generate networks as described before is the use of mesh generators as they are implemented in every commercial finite element program to produce a mesh consisting of tetrahedral element only. In a second step one truss element is to be attached to each edge of each tetrahedral element. A typical example of such networks is shown in Fig. 1. Fig. 1a shows the meshed geometry of a rubber boot applied for example in the automobile industry to protect joints. (Due to the shape of the geometry it is possible to use the symmetry condition, therefore we work only with one half of the rubber boot.) The geometry is loaded on the top by a pressure load P and a bending moment M. Fig. 1b gives a description of the deformed geometry. This small example shows the possibilities to model arbitrary geometries.

In contrast to earlier concepts (see e.g. [10, 14] and [23]) the present method offers the possibility to include non-affinity, arbitrary chain arrangements, inelastic material behaviour and finally the possibility to simulate filled polymer networks (cp. [1] and [24]).

The paper is structured as follows. Section 2 gives a short introduction into the derivation of the finite element formulation which is used in this approach. Detailed information about the derivation can be found in [1]. In Section 3 the proposed model is validated. Therefore we first compare our results with experimental data taken from Treloar [25] and with other simulation data achieved with alternative statistically-based material laws. In a second step the presented concept is applied to three different rubber mixtures. The paper closes with a summary.

2. Finite element formulation

The finite element unit cell consists of one tetrahedral element and six truss elements lying on each edge of the tetrahedral element, see Fig. 2. Due to the fact, that the truss elements as well as the tetrahedral elements have the same number of degree-of-freedoms per node, the assembling procedure of the unit cell is possible and easy to realize. According to the split into one tetrahedral element and six truss elements the Helmholtz free energy function of the unit cell can be additively split into a tetrahedron part (W_{tetr}) and one part coming from the truss elements ($W_{\text{truss}\,j}$ $j = 1, \ldots 6$):

$$W = \underbrace{\frac{\Lambda}{4}\left(J^2 - 1 - 2\ln J\right)}_{W_{\text{tetr}}} + \sum_{j=1}^{6} \underbrace{\frac{1}{A_{0\,j}\,L_{0\,j}} f_{\text{chain}} k\, n_j \Theta \left[\frac{\lambda_{\text{chain}\,j}}{\sqrt{n_j}}\beta_j + \ln\frac{\beta_j}{\sinh\beta_j}\right]}_{W_{\text{truss}\,j}} \tag{1}$$

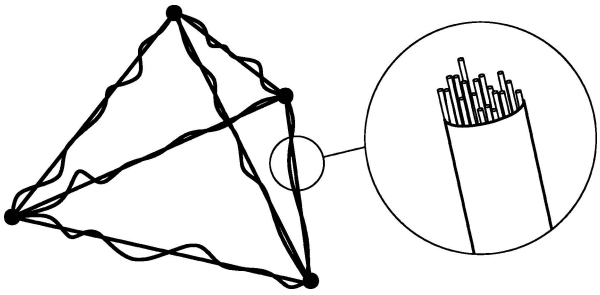

Figure 2 Finite element unit cell with one tetrahedral element and six truss elements. Enlarged: f_{chain} chains per truss element.

In Equation 1 the first summand W_{tetr} of the split, originally introduced by [26] and investigated in further detail by [27], describes the energy function of the tetrahedral element. Here $J = \det \mathbf{F}$ is the determinant of the macroscopic deformation gradient $\mathbf{F}$ and Λ denotes the Lamè constant. This part of the unit cell takes care of the volumetric stiffness. The second part of Equation 1 ($W_{\text{truss}\,j}$) represents the contribution of the polymer chains. Here $\lambda_{\text{chain}\,j} = r_j/r_{0\,j} = L_j/L_{0\,j}$ denotes the stretch of the single chain (micro scale) as well as the stretch of the truss element (macro scale). The assumption that the chain stretch is equal to the truss stretch marks the point of the micro-macro transition. The parameter k denotes the Boltzmann's constant, n_j the number of segments of chain j and Θ the absolute temperature. The inverse Langevin function β can be described in form of a series expansion with different numbers of approximation terms (here called TA). This number of approximations terms contributes to the quality of the approximation, depending on the deformation state. For more details of these parameters see [1]. It is also possible to use other approximations like the Padé approximation e.g. used in [28].

Further unknown in Equation 1 are the cross-section $A_{0\,j}$ and the length $L_{0\,j}$ of the undeformed truss element. As will be shown in the following (see Equation 3) these quantities can be cancelled. Therefore it is not necessary to carry out the difficult task to choose physically reasonable values for them. It can be considered to be an important advantage of the present concept that the results are independent of $A_{0\,j}$ and $L_{0\,j}$.

An important factor to judge the computational efficiency of the approach is $f_{\text{chain}} = N/N_{\text{truss}}$ which describes the ratio between N, the number of polymer chains per reference volume and N_{truss}, the number of truss elements in the same reference volume. To achieve optimum numerical efficiency the parameter must be chosen as large as possible, i.e. one strives to work with as few truss elements as possible. On the other hand convergence has to be guaranteed, see [1]. This is the case when a further increase of truss elements does not alter the macroscopic result.

To implement the Helmholtz free energy function into the finite element formulation we establish the weak form of the balance of linear momentum (volume force and inertia term being neglected) as

$$g = \sum_{z=1}^{n_z} g_{\text{int}\,z} + g_{\text{ext}} = 0 \tag{2}$$

In Equation 2 n_z denotes the number of unit cells. The term $g_{\text{int}\,z}$ represents the virtual work of the internal forces and g_{ext} the contribution of the external loading. After some calculations the following expression for $g_{\text{int}\,z}$ is obtained:

$$\begin{aligned} g_{\text{int}\,z} = & \underbrace{\delta \mathbf{U}_z^T \, f_{\text{chain}} \sum_{j=1}^{6} \int_{-1}^{1} \mathbf{B}_{\text{chain}\,j}^T \frac{\partial W_{\text{chain}\,j}}{\partial \lambda_{\text{chain}\,j}} \frac{1}{2} \, d\xi_j}_{g_{\text{int}\,z}^{\text{truss}} := \delta \mathbf{U}_z^T \, \mathbf{R}_z^{\text{truss}}} \\ & + \underbrace{\delta \mathbf{U}_z^T \mathbf{B}_{\text{tetr}\,0}^T \left. \frac{\partial W_{\text{tetr}}}{\partial J} \right|_0 V_{0\,z}}_{g_{\text{int}\,z}^{\text{tetr}} := \delta \mathbf{U}_z^T \, \mathbf{R}_z^{\text{tetr}}} \end{aligned} \tag{3}$$

In Equation 3 the vector $\mathbf{U}_z$ contains the corresponding twelve degrees-of-freedom. The matrix $\mathbf{B}_{\text{chain}\,j}$ depends on the derivatives of the three displacement components u, v and w (interpolated by linear shape functions), for more details see [29]. Analogous to $\lambda_{\text{chain}\,j} = \mathbf{B}_{\text{chain}\,j} \, \mathbf{U}_z$, the quantity J is expressed by

Table I Different strain energy functions with optimized parameters

model	strain energy function	parameters
Wang-Guth (Wang & Guth 1952)	$W_{\text{WG}} = \frac{Nk\Theta}{3}\sqrt{n}\left[\lambda_1\beta_1 + \sqrt{n}\left(\frac{\beta_1}{\sinh\beta_1}\right) + \lambda_2\beta_2 + \sqrt{n}\left(\frac{\beta_2}{\sinh\beta_2}\right) + \lambda_3\beta_3 + \sqrt{n}\left(\frac{\beta_3}{\sinh\beta_3}\right)\right] + \frac{\Lambda}{4}(J^2 - 1 - 2\ln J)$ $\beta_i = \mathcal{L}^{-1}\left(\frac{\lambda_i}{\sqrt{n}}\right)$, for $i = 1, 2, 3$	$Nk\Theta = 0.03336\,\text{N/mm}^2$ $n = 88.2$
Flory-Rehner (Flory & Rehner 1943)	see remarks in the text	$Nk\Theta = 21.78\,\text{N/mm}^2$ $n = 63$
Arruda-Boyce (Arruda & Boyce 1993)	$W_{\text{AB}} = Nk\Theta\sqrt{n}\left[\beta_{\text{chain}}\lambda_{\text{chain}} + \sqrt{n}\ln\left(\frac{\beta_{\text{chain}}}{\sinh\beta_{\text{chain}}}\right)\right] + \frac{\Lambda}{4}(J^2 - 1 - 2\ln J)$ $\beta_{\text{chain}} = \mathcal{L}^{-1}\left(\frac{\lambda_{\text{chain}}}{\sqrt{n}}\right)$	$Nk\Theta = 0.3\,\text{N/mm}^2$ $n = 26.4$
subnetwork (Wu & van der Giessen 1993)	$W_{\text{SN}} = (1-\rho)W_{\text{WG}} + \rho W_{\text{AB}} + \frac{\Lambda}{4}(J^2 - 1 - 2\ln J)$	$Nk\Theta = 0.3001\,\text{N/mm}^2$ $n = 36.1$ $(\rho = 0.62)$

$J = \mathbf{B}_{\text{tetr}}\,\mathbf{U}_z$, where the vector $\mathbf{B}_{\text{tetr}}$ is a function of the so-called tetrahedral coordinates (cp. [30]).

3. Validations

3.1. Comparison with statistically-based models based on Treloar's data

In this section we compare the results of the proposed approach with the ones of other well-known statistically-based material laws (see Table I) using experimental measurements. For the first comparison we use the data of Treloar for vulcanized rubber [25]. Three deformation states were investigated: uniaxial tension, pure shear and biaxial tension. To enforce (near-)incompressibility the penalty method is used. Due to the fact that we do not present the statistical models in the volumetric-deviatoric decoupled form, the penalty parameter is here the Lamè constant Λ. A good choice for it is 1000 N/mm^2. In Table I the Helmholtz free energy functions of the used material models are listed. The first model was introduced by Wang and Guth [23]. It consists of three orthogonal non-Gaussian chains which deform affinely with the imposed bulk deformation (cp. Fig. 3a). The authors use the Langevin statistics to account for large stretches.

A four chain regular tetrahedron model was proposed by Flory and Rehner [11] for Gaussian chains linked together at the center of a regular tetrahedron, see Fig. 3b. The free ends of the four chains form the corner of the tetrahedron and deform affinely. If the junction point is stationary, the deformation is affine and the Helmholtz free energy function is equivalent to the one of the well-known Neo-Hooke model. Treloar [31] extended the system to include non-Gaussian chains. In this model the junction point of the network is allowed to deform non-affinely, i.e. the position of the junction point is *not* necessarily at the center of the tetrahedron and cannot be easily described analytically. Therefore an explicit expression for the Helmholtz free energy function of the entire network is not available.

To overcome the problem we follow the procedure of Treloar [32] which is based on the idea that the "moving" junction point seeks an equilibrium position if one assumes that there is no net force acting on the junction point. Solving this additional equation by means of the Newton-Raphson scheme it is possible to calculate an incremental stress-stretch relation which characterizes the response of the network.

The third network model is the Arruda-Boyce model [14]. Here eight non-Gaussian chains are linked together in the middle of a cube, see Fig. 3c. Independent

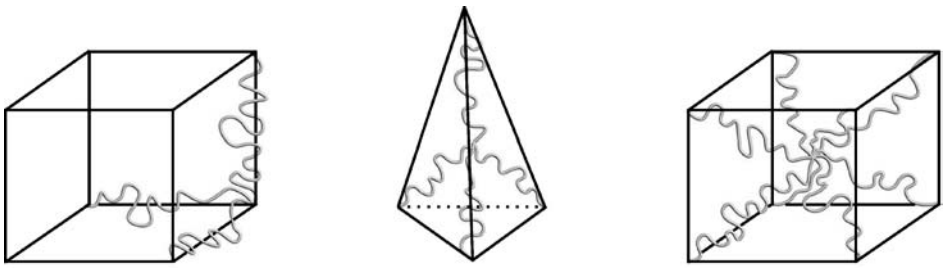

Figure 3 Geometrical illustration of network models: (a) Wang-Guth model, (b) Flory-Rehner model, (a) Arruda-Boyce model.

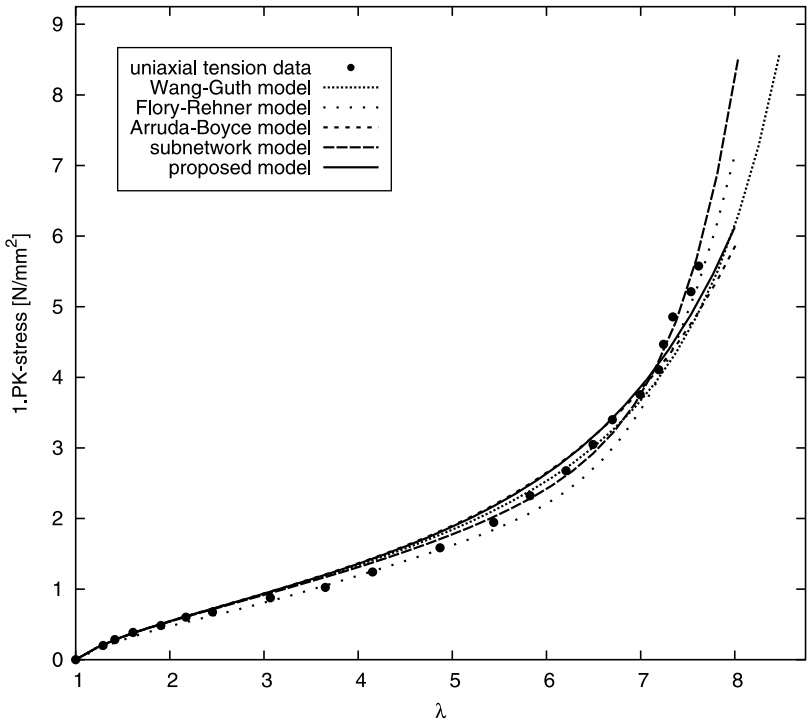

Figure 4 Results of the uniaxial tension simulations.

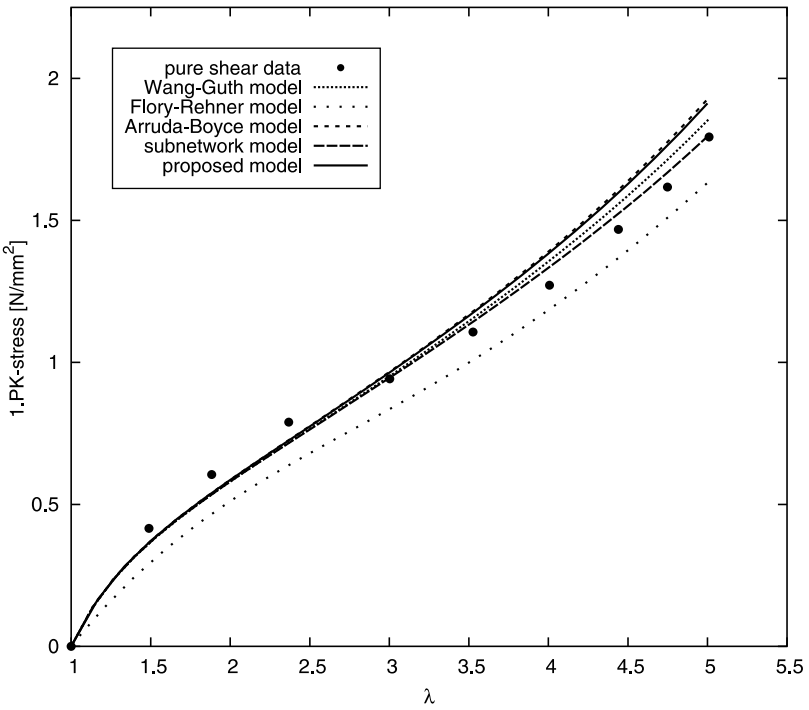

Figure 5 Results of the pure shear simulations.

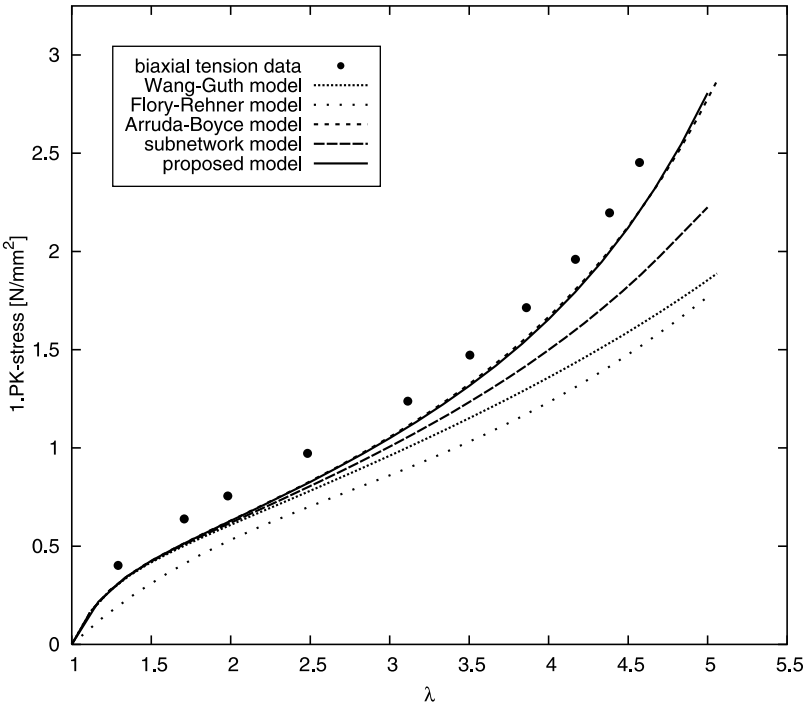

Figure 6 Results of the biaxial tension simulations.

of the deformation state the affinely deforming chains are loaded by tension.

Motivated by the fact that the Wang-Guth model overestimates the stiffness of the network while the Arruda-Boyce model gives a lower bound, Wu and van der Giessen established a so-called subnetwork model [33] and [34]. In Table I the Helmholtz free energy function of this model is shown. The approach uses two material parameters and another parameter ρ to model a linear combination of the Wang-Guth model and the Arruda-Boyce model.

The material parameters of the different models (cp. Table I) are determined by means of a fitting procedure where all three deformation states are taken into account simultaneously. The parameters of the present approach read $n = 5.1$ and $N = 7.975 \cdot 10^{16}\,\mathrm{mm}^{-3}$. Further we work with $N_{\mathrm{truss}} = N/f_{\mathrm{chain}}$ truss elements ($f_{\mathrm{chain}} = 8.968 \cdot 10^{12}$) and 7 terms in the Langevin function. The penalty parameter Λ is set to be equal to $1000\,\mathrm{N/mm}^2$. In all simulations k and Θ are equal to $1.380662 \cdot 10^{-20}\,\mathrm{Nmm/K}$ and 273 K, respectively.

In the following figures the abscissae represents the extension in form of the stretch λ and the ordinate the 1. Piola-Kirchhoff stress defined as force divided by the area of the unstrained cross-section. At first we compare the uniaxial tension simulations with the experimental data, see Fig. 4. Here all models show good agreement with the experimental data.

The results of the pure shear test are plotted in Fig. 5. Here the Flory-Rehner model exhibits in general a too soft material behaviour. The other models underestimate the stress in the small strain regime whereas in the large stretch domain too high stress values are observed. However, the overall agreement with the data can be considered to be satisfactory.

The last experiment to be investigated is the biaxial tension test. The results are plotted in Fig. 6. In comparison to the pure shear deformation state the Flory-Rehner model again shows a too soft material response. This fact is, although not to such an extent as for the Flory-Rehner model, also exhibited by the Wang-Guth model and the subnetwork model. The best agreement is achieved by the Arruda-Boyce model and the proposed approach. Furthermore these two concepts show a similar material behaviour.

In general it can be said that the Arruda-Boyce model and the proposed model are able to reproduce the material response of the experiments in all three deformation states in a good manner, especially if one takes into account that these models depend on only two material parameters. For the deformation states uniaxial tension and pure shear all models, with exception of the Flory-Rehner model in the pure shear experiment, show more or less good agreement with the experimental data and among each other. Only in the biaxial tension test, with exception of the Arruda-Boyce model and the proposed model, all models exhibit dissatisfactory correlation with the data.

3.2. Comparison with experimental data of three different rubber compounds

For the second validation we use experimental data of Arruda and Boyce [14]. The authors carry out uniaxial compression tests and plane strain compression tests for three different rubber mixtures. The deformation states uniaxial compression and plane strain compression represent extremes in the behaviour of polymer networks. In the uniaxial compression test the specimen is stretched in all directions perpendicularly to the load direction. For the plain strain compression test the material is held within a channel which constrains the specimen in such a way that only one direction is free to move.

Table II Material parameters for three different mixtures

	n	N [mm^{-3}]	f_{chain}
silicon rubber	1.03	$6.683 \cdot 10^{16}$	$1.0 \cdot 10^{13}$
gum rubber	30.9	$6.383 \cdot 10^{16}$	$9.566 \cdot 10^{12}$
neoprene rubber	78.3	$1.677 \cdot 10^{17}$	$2.513 \cdot 10^{13}$

Three different rubber compounds were chosen in this study. The first one is a silicon rubber, the second one a gum rubber and the last one a neoprene rubber. For more details of the experimental set-up and the measurement procedure see [14]. In order to compare our model with these experiments we chose for all three mixtures two terms in the Langevin function and the penalty factor reads $\Lambda = 1000\,\text{N/mm}^2$. The parameters are listed in Table II. In the fitting procedure only the uniaxial compression test was used.

The results of the simulations in comparison with the experiments are shown in Fig. 7. The proposed approach accurately captures the deformation states of all three materials. If one compares the material response of the uniaxial compression test and the plane strain compression test of all three materials it is obvious that the materials are noticeably different with regard to stiffness and limiting extensibility. The latter aspect

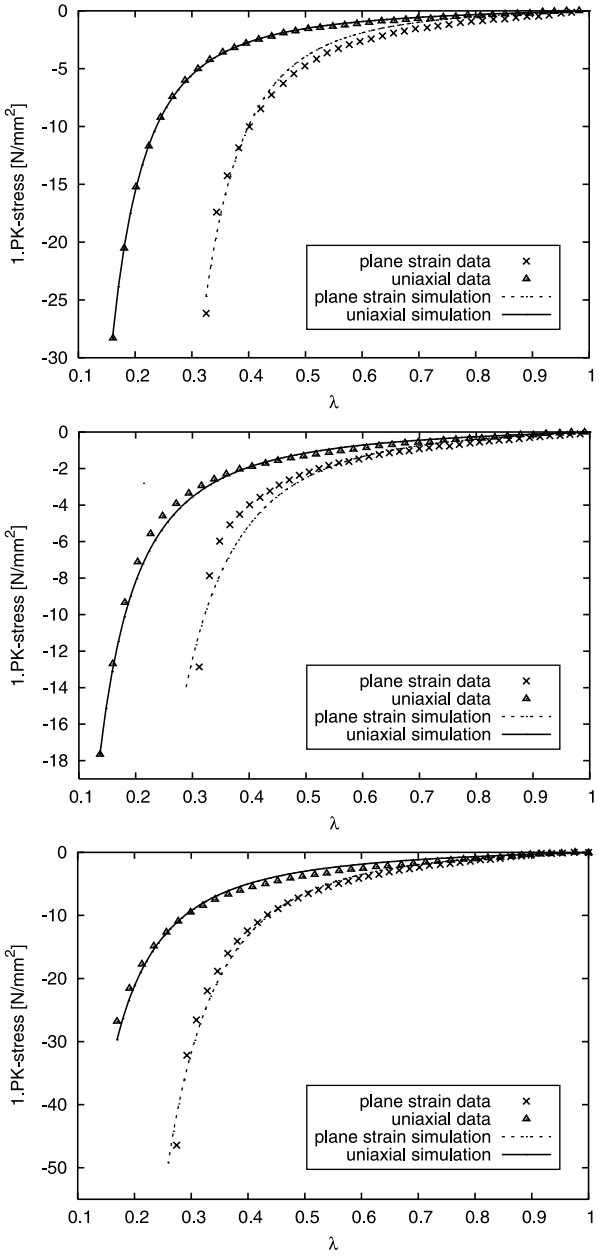

Figure 7 Comparison between simulations and experiments: (a) silicon rubber, (b) gum rubber, (c) neoprene rubber.

can be seen as an additional validation of the suggested method.

4. Summary

In the present paper we have proposed a micro mechanically-based finite element concept to model the deformation behaviour of rubber-like materials. The main advantage of the suggested concept is that only physically-based parameters are used. The suggested method emanates from the idea that these parameters, namely the number of chain links (n) and the number of chains per reference volume (N), are easily provided by the polymer chemist who designs the mixture.

The emphasis of the work lies on the validation by means of experimental data. In the first step the correlation of the modelling results with experimental data of a vulcanized rubber in three different deformation states is investigated. In comparison to other statistically-based material models it has been found that the Arruda-Boyce model and the proposed model are clearly superior to the other employed approaches.

In the second step the parameters of the here shown concept are adjusted to three different rubber mixtures. The highly satisfactory agreement of the numerical and the experimental data illustrates the capability and the effectiveness of the proposed approach.

References

1. M. BÖL and S. REESE, *Intern. J. Solids Struct*.
2. R. J. GAYLORD, *Poly. Engng. Sci.* **19**(4) (1979) 263.
3. J. GAO and J. H. WEINER, *Macromolecules* **24**(18) (1991) 5179.
4. A. S. LODGE, An Introduction to Elastomer Molecular Network Theory (The Bannatek Press, Madison).
5. M. WITTKOP, J. U. SOMMER, S. KREITMEIER and D. GÖRITZ, *Phy. Rev. E* **49**(6) (1994) 5472.
6. T. HÖLZL, H. L. TRAUTENBERG and D. GÖRITZ, *Phys. Rev. Lett.* **79**(12) (1997) 2293.
7. M. LANG, D. GÖRITZ and S. KREITMEIER, Constitutive Models for Rubber III, edited by J. J. C. Busfield and A. H. Muhr (2003) p. 195.
8. W. KUHN, *Kolloid-Zeitschrift* **76**(3) (1936) 258.
9. F. T. WALL, *J. Chem. Phys.* **10** (1942) 485.
10. P. J. FLORY, and B. ERMAN, *Macromolecules* **15**(3) (1982) 800.
11. P. J. FLORY and J. REHNER, *J. Chem. Phys.* **11**(11) (1943) 512.
12. L. R. G. TRELOAR, *Trans. Fara. Soc.* **39**(1943) 36.
13. L. R. G. TRELOAR, *ibid.* **39** (1943) 241.
14. E. M. ARRUDA and M. C. BOYCE, *J. Mech. Phys. Solids* **41**(2) (1993) 389.
15. J. E. BISCHOFF, E. A. ARRUDA and K. GROSH, *J. Appl. Mech.* **69** (2002) 570.
16. P. D. WU and E. VAN DER GIESSEN, *J. Mech. Phys. Solids* **41**(3) (1993) 427.
17. L. ANAND, *Comp. Mech.* **18** (1996) 339.
18. W. KUHN and F. GRÜN, *Kolloid-Zeitschrift* **101**(3) (1942) 248.
19. M. MOONEY, *J. Appl. Phys.* **11** (1940) 582.
20. R. S. RIVLIN, *Philosop. Trans. Royal Soc. London* **A240** (1948) 459.
21. R. W. OGDEN, *Proc. Royal Soc. London A* **326** (1972) 565.
22. S. R. SWANSON, *J. Engng. Mater. Technol.* **107** (1985) 110.
23. M. C. WANG and E. GUTH, *J. Chem. Phys.* **20**(7) (1952) 1144.
24. S. REESE and M. BÖL, Constitutive Models for Rubber III, J. J. C. Busfield and A. H. Muhr (2003) 213.
25. L. R. G. TRELOAR, *Trans. Fara. Soc.* **40** (1944) 59.
26. R. W. OGDEN, *Proc. Royal Soc. London A* **328** (1972) 567.
27. J. C. SIMO, Handbook of Numerical Anylysis, vol. III, edited by R. S. Ciarlet and J. L. Lions, Elsevier, Amsterdam.
28. C. MIEHE, S. GÖKTEPE and F. LULEI, *J. Mech. Phys. Solids* **52** (2004) 2617.
29. P. WRIGGERS, Nichtlineare Finite-Element-Methoden (Springer, 2001).
30. O. L. ZIENKIEWICZ and R. L. TAYLOR, The Finite Element Method, Vol. I: The Basis (Butterworth-Heinemann).
31. L. R. G. TRELOAR, *Trans. Fara. Soc.* **42** (1946) 83.
32. L. R. G. TRELOAR, *ibid.* **50** (1954) 881.
33. P. D. WU and E. VAN DER GIESSEN, *Mech. Res. Commun.* **19**(5) (1992) 427.
34. P. D. WU and E. VAN DER GIESSEN, *Philosop. Magazine A* **71**(5) (1995) 1191.

Received December 2004
and accepted April 2005